

Influence of Ultrasound on Embossing Results for Cardboard

Jennes Hünninger,^{a,b,*} Lutz Engisch,^{a,b} Simon Hamblyn,^{a,b} Ulrike Käppeler,^{a,b} and André Hofmann^c

The requirements for embossing of cardboard for print and packaging applications are constantly increasing. High degrees of forming, richness of detail, and high shape accuracy are desired. However, current embossing technology can only fulfil these requirements to a limited extent. A loss of detail and moderate degrees of forming are typical defects in the embossing process. In previous research work, a positive effect on the forming behavior of cardboard could be observed by the application of ultrasound. Therefore, the influence of ultrasound was also investigated for embossing. In order to quantify the effects of ultrasound, conventional and ultrasonic-assisted embossing results were compared. New approaches for analysis and evaluation of embossing results and new characteristic values for describing the forming were applied for the comparison. Two exemplary embossing geometries and a range of ultrasonic parameters were used to characterize the impact of ultrasound and showed positive effects to the forming results.

DOI: 10.15376/biores.17.4.5803-5819

Keywords: Embossing; Cardboard; Ultrasound; Shape accuracy; Forming behavior

Contact information: a: Leipzig University of Applied Sciences (HTWK Leipzig), Faculty of Computer Science and Media, P.O. Box 301166, 04251 Leipzig, Germany; b: iP³ Leipzig - Institute for Printing, Processing and Packaging Leipzig, P.O. Box 301166, 04251 Leipzig, Germany; c: Technical University of Dresden (TU Dresden), Institute of Natural Materials Technology, Bergstraße 120, 01189 Dresden, Germany; *Corresponding Author: jennes.huenniger@htwk-leipzig.de

INTRODUCTION

The highlighting of the individuality of products as well as the creation of a special look and feel are today key components in a brands marketing strategy to ensure that a product stands out on a shelf amongst products from its competitors. Therefore, the finishing of printed products and packaging is an important part of manufacturing process, and embossing is a key technology for the production of high-quality and multi-sensory surfaces. The requirements for embossing of cardboard have increased rapidly, but they can only be implemented in practice to a limited extent. The use of ultrasound in paper production and in the forming of paper and other fiber-based materials has been the focus of several research studies and has been shown to provide a positive effect on the forming results. Therefore, it is suspected that the application of ultrasound in the embossing process can achieve an increase of the degree of forming, as well as improving detail and shape accuracy. The evaluation of embossing results is currently largely based on visual inspection. There are no standardized geometries and values for an objective evaluation of embossed structures. Therefore, new approaches for objective analysis and evaluation were first developed to compare ultrasonic-assisted embossing with conventional embossing.

The evaluation of embossing is done visually in terms of accuracy and positioning (Tenzer 1989; Blechschmidt 2013). The dimensional and shape accuracy is compared with an undefined reference. Tenzer (1989) defined geometric quantities for embossed samples, for example depths, flank angles, and radii of rounding at the edges of the embossing element. The difference in the material thickness under load and after load release is called re-swelling. This occurs due to the viscoelastic nature of materials such as cardboard, which recover some of their thickness lost due to compression forces over time. Systematic studies on the embossing process exist only in rudimentary form. The influence of embossing pressure, time, temperature, material properties, and embossing geometry on the embossing result is known (Liebau and Heinze 2001; Bos and Staberock 2006). But the interactions have not been quantified yet due to the lack of standardized analysis and evaluation methods. The embossing force, a machine parameter used to control the process, is one of the main influencing factors. But this force is distributed locally differently over the whole forming system. The distribution will change during the embossing process in dependency of the contact between the embossing tools and the cardboard and the degree of forming. The force depends on the properties of the cardboard and the embossing geometry. The active pressure within the forming system cannot be determined in a spatially resolved manner. Hünninger (2013) used FUJIFILM Prescale pressure measurement film to determine the pressure distribution during embossing. However, the results only show the pressure distribution, not the locally acting pressures. To analyze the embossing results, the embossing height was measured as specific values and compared with the embossing tool. Because of the disadvantages of embossing force described above, Hünninger (2013) used the penetration depth of the embossing tool into the cardboard sample, hereby defined as the embossing path, as relevant process control value instead of the total force applied.

Researchers of the Technical University of Dresden have been analyzing the forming behavior of cardboard during the deep-drawing for the production of hollow bodies for many years. And although the dimensions, requirements, and parameters differ from the forming while the embossing process, there is some transferability of knowledge in the analysis and evaluation methods that can be used. These include definitions of quality criteria and relevant geometric parameters such as lengths, radii, and angles of the forming results (Hauptmann 2010; Wallmeier 2018). Zahel and Schaffrath (2018) as well as Grenz and Schramm (2018) evaluated the forming results using a grading system related to the number of folds, the crack length, and the presence of micro cracks in the surface. The formed shape was analyzed with surface measurements techniques such as stripe light projection with a subsequent image evaluation and visual inspection.

Ultrasound has been used in the paper industry since 1950 for influencing fiber properties (*e.g.* Jayme and Rosenfeld 1955; Laine and Goring 1977) and for deinking in the recycling of waste paper (*e.g.* Turai and Teng 1979). In addition, ultrasound can be used for bonding and strengthening paper and board webs (Gmeiner 2001; Gmeiner and Schneider 2005) and for smoothing board surfaces (Wanske 2010). The use of ultrasound in the forming of cardboard was investigated as part of the studies on the deep-drawing of cardboard. Different ultrasonic parameters and their influence on the forming quality as well as the interaction between material and tool were investigated (Loewe *et al.* 2017a). It was shown that the use of ultrasound results in a reduction of the punch force of 80 % compared to the conventional deep-drawing process. This reduction in force was attributed to a minimization of friction between the tool and the material as a result of the material compression and the cyclical change of the gap conditions during the

deep-drawing process. Furthermore, an increase in the surface smoothness of ultrasonically deep-drawn specimens was observed (Loewe *et al.* 2017b). The application of ultrasound during forming causes a temperature increase within the cardboard, which may have a positive effect on forming results (Loewe *et al.* 2019; Hofmann and Hauptmann 2020).

Heated embossing tools have been shown to have a positive effect on the embossing results (Tenzer 1989; Liebau and Heinze 2001). The tool temperature affects the degree of forming, the compensation of surface structures, and the shape accuracy of the embossing. Ultrasound causes heating inside the fiber network. The investigation of the thermal influence on the mechanical properties of cardboard while ultrasonic-assisted embossing shows a degreasing of the splitting strength and bending stiffness and an increasing of compressibility (Käppeler *et al.* 2020). This could lead to a better forming result with ultrasonic-assisted embossing, because the cardboard properties influence the embossing resistance. A change in the chemical composition and morphological properties of cardboard due to the energy input of ultrasound could not be demonstrated (Käppeler *et al.* 2021). Hofmann and Hauptmann (2020) showed that the influence of ultrasound on the dynamic material compression depends on the specific material properties of the cardboard used. Due to burns in the material, there are limits to the ultrasonic application. In addition, hollow formations were observed within the cardboard layers, which are presumably related to the evaporation of water contained in the fiber structure. Radzanowski (2017) compared in first basically investigations conventional with ultrasonic-assisted embossed samples and showed that higher embossing depths can be achieved by ultrasound and that significantly less embossing force is required to achieve comparable embossing depths by ultrasound.

The reported effects in the literature for ultrasonic-assisted treatment and forming of cardboard indicate that the use of ultrasound and the associated additional material compression in relation with heating inside the material represents a potentially useful technological enhancement for the embossing process. Thus, the aim of this work was to investigate the influence of ultrasound on embossing results. The approach of using the embossing path rather than the process force makes it possible to analyze the effects of process, material, and embossing geometry independently.

EXPERIMENTAL

Embossing

To compare the results of conventional and ultrasonic-assisted embossing, a series of experimental investigations were carried out. Test elements with defined shapes and geometries were selected for the embossing. It was known from previous experiments that embossing geometries with sharp-edged shapes have a different forming behavior than geometries with soft gradients. Therefore, a truncated pyramid with a flank angle of 45° (sharp-edged shape) and a spherical cap (soft gradient shape) were used. The test elements had an element height of 600 µm and an edge length or diameter of 6 mm. The embossing tests were made with a conventional coated folding carton (Performa Bright, Stora Enso), which consisted of a three-layer fiber construction, a triple-pigment-coated top side, and an uncoated reverse side. The cardboard had a grammage of 320 g/m² and a material thickness of 551 µm ± 4 µm according to DIN EN ISO 534 (2012).

For the conventional and ultrasonic-assisted embossing processes, the test setup consisted of an embossing tool with a relief embossing geometry and a flat counter tool. The cardboard sample was positioned between them. One tool is driven towards the other, and the embossing process begins when both tools are in contact with the surface of the cardboard sample, therefore applying a pressure on the cardboard surface. As the distance between the embossing tools is further reduced, the embossing element is driven deeper into the cardboard surface until a specified maximum force or embossing path is reached. The forming of the embossing relief into the surface of the cardboard is achieved primarily by material compression. The path change from the initial contact position to the end of the process is defined as the embossing path, which corresponds to the penetration depth of the embossing tool into the cardboard sample during the forming process and is hence the embossing depth under load. The process steps and the connection of the parameters are shown in Fig. 1.

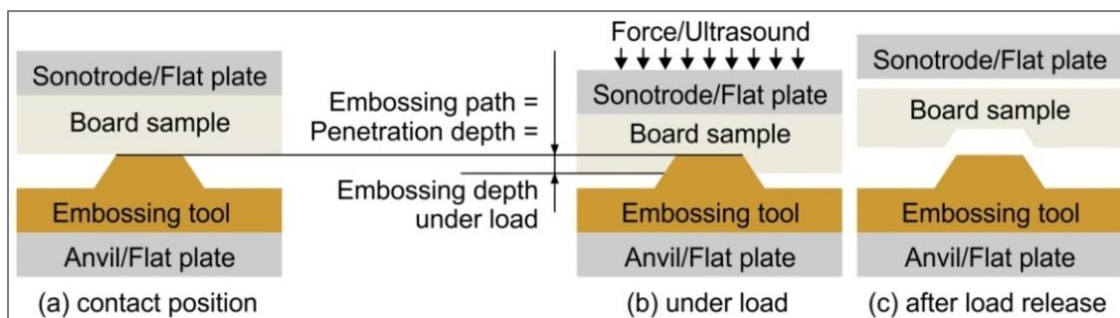


Fig. 1. Contact position (a), under load (b) and after load release (c) and context of embossing path, immersion depth and embossing depth under load

The experiments using ultrasonic-assisted embossing were carried out first using a laboratory testing machine (Fig. 2). The specifications of the test rig were published previously (Hofmann and Hauptmann 2020).

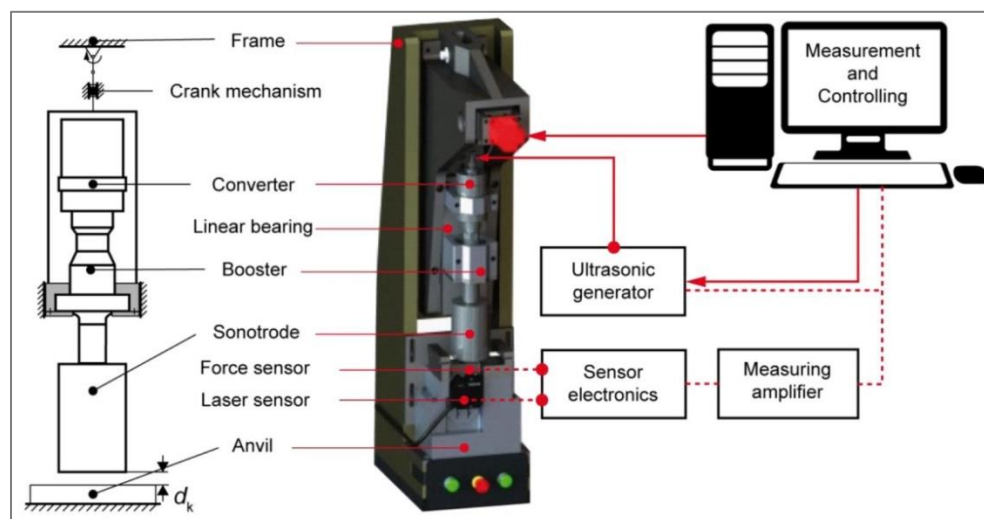


Fig. 2. Test rig for ultrasonic-assisted embossing (Hofmann and Hauptmann 2020)

The embossing tools were CNC-milled from brass and were fixed at the anvil using a double-sided tape. The process parameters ultrasonic amplitude and embossing force were varied, and the resultant embossing path was measured using a laser.

The conventional embossing tests were carried out on a Materials Testing Machine (Zwick Roell, Germany, Ulm) with a special embossing module. The embossing module was made of two plane-parallel plates that were connected via a sliding shaft and sleeve system containing linear motion bearings to ensure parallel travel of the plates with a smooth low friction motion (Fig. 3).

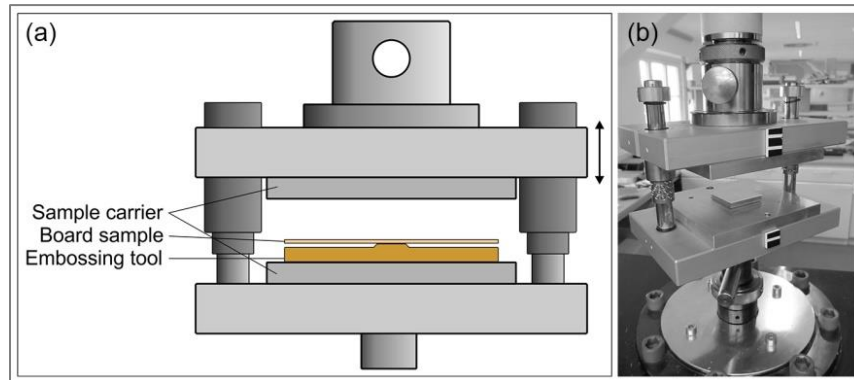


Fig. 3. Test setup (a) and embossing module at the Zwick Testing Machine (b)

The embossing tool was fixed to one of the flat aluminum sample carriers using a double-sided tape, while the other sample carrier was used as the counter tool. The test speed was set of 5 mm/min. The end of the process was set by a defined maximum embossing path. The embossing path was measured using a non-contact extensometer (Zwick Roell, Germany, Ulm). The specifications are based on the measured embossing paths while ultrasonic-assisted embossing. The cardboard samples were stored in a standard climate (23 °C and 50% r. H.) according to DIN EN 20187 (1993) before, during, and after forming. Five embossed samples were evaluated for each variation.

Sample Characterization

The topography of the embossing tools and the embossed cardboard samples were measured with a stripe light projection instrument (3D-Macroscope VR-3100, Keyence Deutschland GmbH, Neu-Isenburg, Germany) with a 12x magnification. This produced a measurement area of 24 mm x 18 mm. Therefore, the embossed shapes and a part of the non-formed surfaces surrounding it were contained within the measurement field. The analysis was made on profiles of cross-sections and depended on the embossing geometry. Hence, the different test elements were considered separately. Typical profiles and characteristic values for the spherical cap embossing tool and an embossed cardboard sample are shown in Fig. 4.

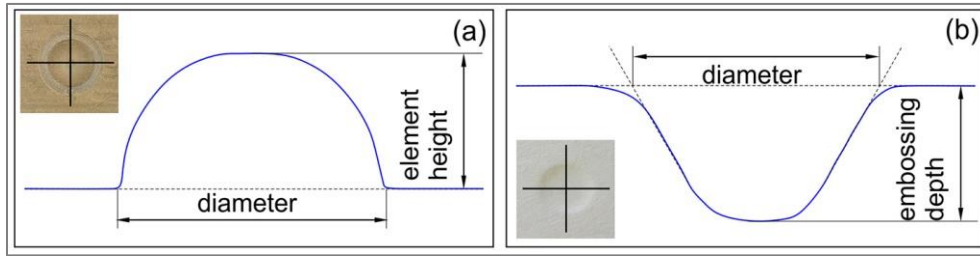


Fig. 4. Cross sections and characteristic values of the embossing tool (a) and the embossed samples (b) of spherical cap

The spherical cap was characterized by a round gradual shape with the highest point in the center of the diameter. The embossing tool had a raised element with sharp lower edges, where the element met the surrounding area. The embossed samples had an impressed form, with softer edges. A cross-sectional profile in the horizontal and vertical directions was used. The element height/embossing depth were measured at the left and right side of the embossing element on each profile. Therefore, each measurement resulted in two measured values per direction for the element height/embossing depth and one measured value per direction for the diameter. The mean value was calculated based on 5 embossed samples for each direction.

The truncated pyramid was characterized by sharp edges with defined flank angles and lower and upper edge lengths. Due to its quadratic form, three horizontal and three vertical cross-section profiles were used. For each profile, the element height/ embossing depth and flank angles were measured on both sides of the profile, while single measurements were made for the upper and lower edge lengths (Fig. 5).

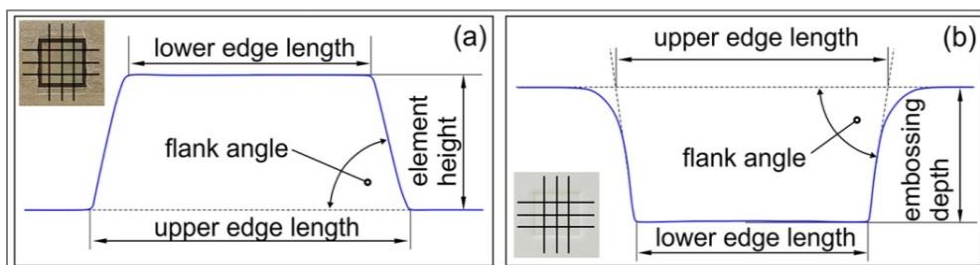


Fig. 5. Cross sections and characteristic values of the profile curve of the embossing tool (a) and the embossed samples (b) of truncated pyramid

Therefore, the measurement resulted in six measured values per direction for the element height/embossing depth and flank angles and three measured values per direction for the upper and lower edge lengths. The results from the 3 sets of measurements in each direction were averaged over 5 samples to find the mean and standard deviations.

If the embossing path is smaller than the element height, then the embossing tool is not completely immersed in the cardboard sample. Therefore, the acting diameter/ upper edge length of the embossing tool is smaller and has to be measured as a function of the embossing path (Fig. 6 a). The difference of the embossing depth under load and after load release is the characteristic value of re-swelling (Fig. 6 b). The re-swelling represents the elastic behavior of the board sample.

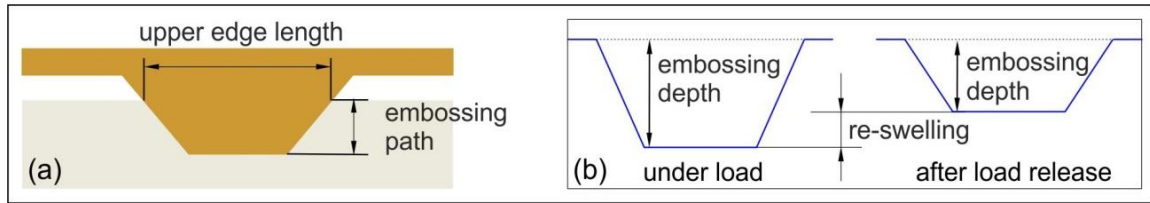


Fig. 6. Analysis of the upper edge length as function of the embossing path (a) and the definition of the characteristic value of re-swelling (b)

To evaluate the quality of the embossed samples, methods to characterize the edge sharpness (Edge Inaccuracy) and the curvature at the base of the embossing (Curve Effect) were developed (Fig. 7).

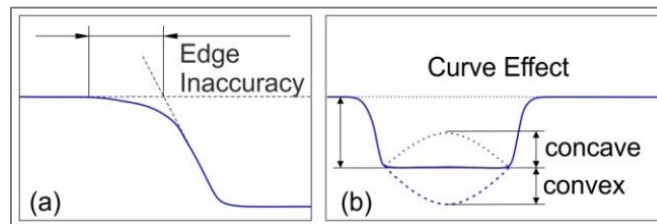


Fig. 7. Edge Inaccuracy (a) and Curve Effect (b) of embossed samples of truncated pyramid

The edges of the embossed samples resulting from both element geometries had less edge sharpness than on the tools and therefore contained deviations from the tool geometry. The radii of the edge rounding on the samples were in fact so large that the center of a projected circle lay outside the measurement field. In addition, the rounded edges of the embossing did not have a consistent radius, and therefore it was not possible to characterize the edge inaccuracy using on a radius-based measurement method.

The Edge Inaccuracy characterization method developed (Fig. 7a) utilizes the deviation of the profile of the upper forming edge on the embossing from that of a sharp edge with the same flank angle. By extending the flank of the embossing up until it intersects the zero plane and marking the point where the edge rounding on the upper forming edge begins, two reference points are defined, which mark the start and end points where the edge deviates from being sharp to being rounded. The Edge Inaccuracy is the ratio of the sum of the lengths of the edge deviations on both sides of the embossing profile to the diameter/upper edge length of the embossing. Therefore, less rounding results in smaller deviation lengths and hence lower values of Edge Inaccuracy.

The base of the embossed truncated pyramids should be flat, but often the embossing in the cardboard had a small curvature, which was either convex or concave, depending on the experimental conditions used (Fig. 7b). The Curve Effect CE was analyzed by calculating the difference between the embossing depths at the edges to the embossing depth in the center. Tolerances of the curve orientation were set at $\pm 5 \mu\text{m}$, because the surface of the cardboard samples was not perfectly uniform due to small material thickness variations of the cardboard. If the embossing depth in the center was smaller than the embossing depth at the edges ($\text{CE} > 5 \mu\text{m}$), then the center curved upwards (convex). If the embossing depth in the center was larger than the embossing depth at the edges ($\text{CE} < -5 \mu\text{m}$), then the center curved downwards (concave). If there was no difference, i.e. the depth in the center was within $\pm 5 \mu\text{m}$, then the base was deemed to be a flat plain.

RESULTS AND DISCUSSION

To investigate the impact of ultrasound on the embossing, the embossed samples of the conventional embossing (conv) and ultrasonic-assisted embossing with ultrasonic amplitudes of 15 μm (US-15) and 30 μm (US-30) were compared. As stated previously, in the ultrasonic-assisted embossing experiments, the maximum force was used as the control parameter, and the resultant embossing path was measured. It was initially intended that the same embossing paths generated in the ultrasonic-assisted experiments be subsequently used in the conventional embossing experiments, so that direct comparisons could be made. However, the initial experiments showed that this range needed to be significantly extended for the conventional embossing experiments in order to produce visible indentations in the cardboard surface, due to the viscoelastic recovery within the material once the load had been removed. The comparison of the embossing depths relative to the embossing path showed that a much shorter embossing path was generally required when ultrasound was used compared to the conventional process in order to achieve similar final depths in the finished embossing (Fig. 8).

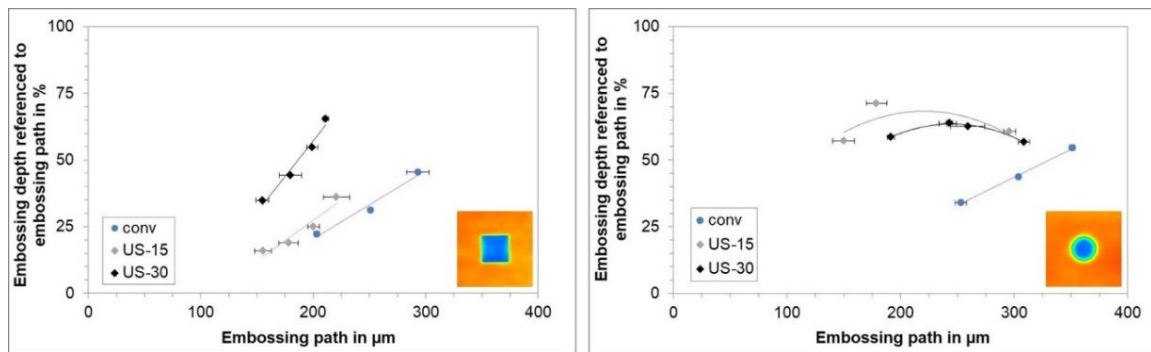


Fig. 8. Embossing depths relative to embossing paths of truncated pyramid and spherical cap

For the truncated pyramid, the correlation between the embossing depth and embossing path was approximately linear for the ultrasonic and conventional processes. With the spherical cap, a maximum embossing depth was achieved with ultrasound. This was presumably due to the maximum compression of the material being achieved, which was not the case with the conventional embossing. With an increase of the embossing depth, the compression state and the compression resistance increased. This therefore shows that in order to achieve a certain depth of an embossed element in the finished product, the use of ultrasound increases the effectiveness of the process, whereby more of the material compression caused by the penetration of the element into the cardboard was converted to plastic deformation. The relationship between the embossing depth and the embossing path give an insight to the amount of out-of-plane plastic deformation and elastic recovery that occurred during the process. Figure 9 shows the embossing depth as a percentage of the embossing path (plastic deformation) compared to the elastic recovery (re-swelling) for a 200 μm embossing path for the truncated pyramid and a 250 μm embossing path for the spherical cap.

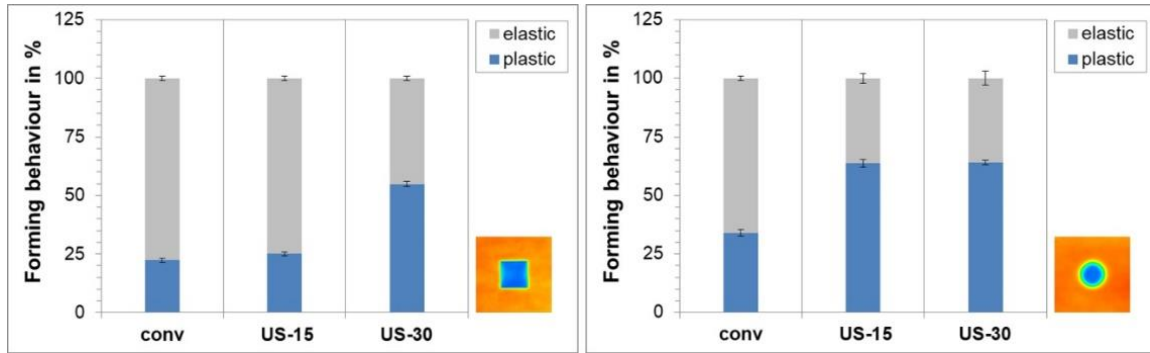


Fig. 9. Comparison of the embossing depth and the re-swelling referenced to the embossing path of truncated pyramids and spherical caps

In the case of the truncated pyramid, for the conventional process less than 25% of the embossing path was converted into plastic deformation and hence the embossing depth after load release, with more than 75% of this embossing depth under load being lost due to elastic recovery (re-swelling). This relationship was also similar for the ultrasonic-assisted embossing with the 15 μm amplitude. However, when a 30 μm amplitude was used, the same embossing path resulted in approximately 55% plastic deformation.

For the spherical cap element, the relationships were different from the truncated pyramid, where overall more plastic deformation occurred for both processes. For the conventional process, the embossing depth after load release was approximately 34% of the embossing depth under load, which means that approximately 66% was lost to re-swelling. For the ultrasonic-assisted embossing, the embossing depth after load release was approximately 64% of the embossing depth under load. Therefore the differences between the conventional and ultrasonic processes were smaller for the spherical cap element than for the truncated pyramid. However, unlike for the truncated pyramid element, the differences in the amount of plastic deformation and elastic recovery were negligible between the two amplitudes of the ultrasonic embossing.

In a conventional cardboard embossing process, as the embossing path and hence the penetration depth increases, the fiber network becomes denser due to the compaction. This increase in density increases the compression resistance, and therefore more force is required for the tool to penetrate further. However, high levels of compactions are required to achieve higher levels of plastic deformation. The higher amounts plastic deformation in the ultrasonic process can partially be attributed to dynamic compaction due to the ultrasonic amplitude (Wanske 2006; Loewe *et al.* 2019), resulting in higher compaction ratios. The heat induced into the fiber network as a result of the ultrasound could also potentially lead to softening of the lignin, which could in turn allow the fibers to be deformed more easily and then frozen into a new position when cooled.

Figure 10 shows the absolute re-swelling, *i.e.* the amount of out-of-plane recovery after the load was removed.

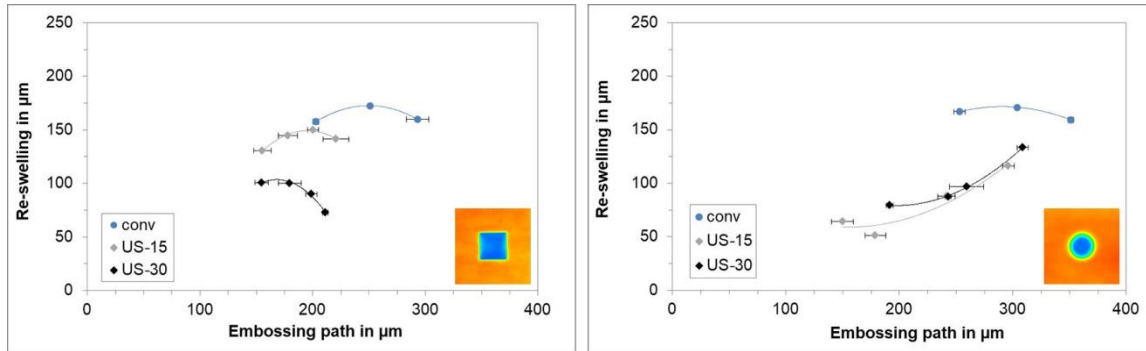


Fig. 10. Comparison of the absolute re-swelling of truncated pyramids and spherical caps

For the truncated pyramid embossed using a 30 μm amplitude, there was an overall decrease in the absolute amount of re-swelling as the embossing path was increased. This shows that the rate of conversion to plastic deformation increased; the deeper the tool was driven into the cardboard. There was also an interaction between ultrasonic energy and embossing path. For the 15 μm amplitude ultrasonic and the conventional embossing, the absolute amount of re-swelling were higher than for the higher amplitude and remained relative constant over the embossing path used, indicating that the amount out-of-plane recovery did not change as the embossing path was increased. However in relative terms, increasing embossing path led to a decrease in the percentage of re-swelling as more absolute plastic deformation occurred.

For the spherical cap element, there was an overall increase in the absolute amount of re-swelling as the embossing path was increased for both amplitudes of the ultrasonic embossing. Notable less absolute re-swelling occurred for shorter embossing path using ultrasonic-assisted embossing, therefore the advantage of using ultrasonic energy decreased as the embossing path increased. However, unlike for the truncated pyramid, little/no difference was observed between the results of the different amplitudes used. For the conventional embossing the absolute amount of re-swelling remained relatively constant over the embossing path used, indicating that the absolute amount out-of-plane recovery did not change as the embossing path increased.

The absolute re-swelling of the conventional and ultrasonic-assisted embossing results of truncated pyramids and the conventional embossing results of the spherical cap reached a maximum and decreased thereafter. For the truncated pyramids, the inner area of the embossing geometry was flat, and therefore the contact pressure distribution was uniform across the width of the element, albeit with less pressure occurring on the flanks. The material compression should therefore be relatively even over the width of the element. Due to the curved shape of the spherical caps, the contact area increased as the embossing path was increased. This resulted in changes to the pressure distribution the deeper the element was impressed into the cardboard, with the highest pressure being applied in the center of the element. Therefore the maximum penetration occurred in the middle of the embossing and decreased towards the edges. Therefore, varying amounts of strain and material compression would occur over the area of the embossing (Fig. 11).

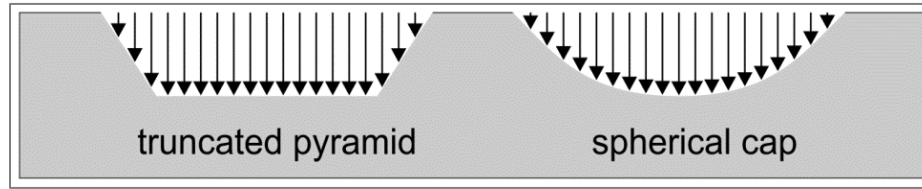


Fig. 11. Difference of material compression related to the embossing geometry

The curvature of the spherical cap element would likely result in less dynamic compression occurring compared to the flatter truncated pyramid, resulting in more localized differences in material compression (Hofmann and Hauptmann 2020) from the spherical cap element. The simultaneous heating and drying of the material resulting from the ultrasonic energy in a loosening of the fiber structure (Käppeler *et al.*, 2021) is likely to result in more voids being present in the fiber network and an increase in the out-of-plane recovery. Therefore in the areas of low compaction, such as near the top of the spherical cap embossing, the use of ultrasonic energy could lead to increases in re-swelling. This needs to be investigated further to better understand the correlation between ultrasound, material compaction and plastic deformation.

To analyze the shape accuracy, the edge lengths/diameter of embossing results were referenced to the embossing tool. The deviations of the embossed samples from the tool were compared in Fig. 12. The upper plane of the truncated pyramid on the embossing tool formed the lower plane in the embossing. This was in contact with the embossed area of the board sample during the entire embossing process.

Because of the continuous contact, the embossed samples of the lower edges lengths were a faithful reproduction of the dimension of the tool, and therefore showing little/no deviation regardless of the path length or ultrasonic conditions used.

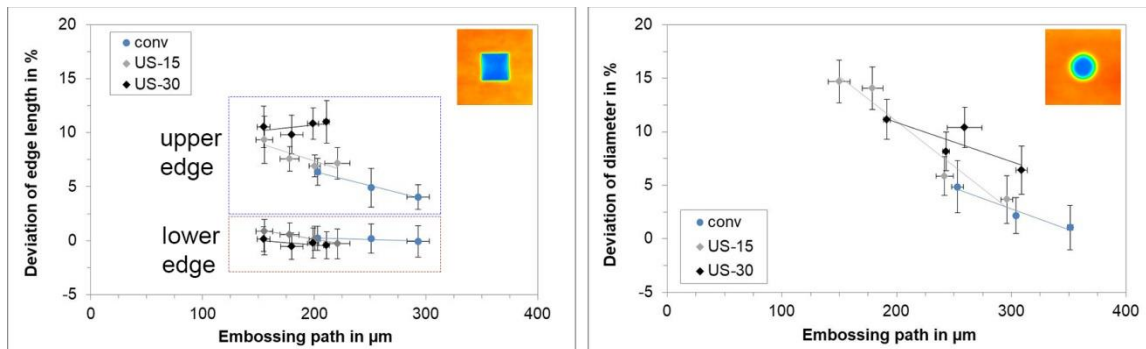


Fig. 12. Deviation of edge length/diameter of the embossed samples referenced to the embossing tool of truncated pyramids and spherical caps

The deviation of the upper edge length of the truncated pyramid decreased with increasing embossing path for the conventional and low amplitude ultrasonic embossing. However, within the range of embossing paths used, the upper edge lengths remained larger than the dimensions of the tool. For the 30 μm amplitude, no reduction in the deviation was observed as the embossing path was increased. For the spherical cap, a reduction in diameter deviation was observed for the ultrasonic and conventional embossing processes as the embossing path was increased (Fig. 12b). However as with the truncated pyramid, the deviations were lower for the conventional process. The higher deviation in upper edge lengths and diameters for the ultrasonic embossing could presumably be explained by

micro-movements of the board samples and the tools in the x-y-dimension, therefore creating wider openings. Loewe *et al.* (2017a) detected movements of the tool in the x-y direction up to 5 μm with an ultrasonic amplitude of 30 μm . With smaller ultrasonic amplitude, the micro-movements became smaller and had less influence on the upper length of the embossing, hence smaller deviations from the lower amplitude. The impact of ultrasound becomes apparent when the results of equal embossing depths are compared (Fig. 13).

For the truncated pyramids, the comparable embossing depth was 79 μm , for the spherical caps approximately 180 μm . The deviations were higher for the ultrasonic-assisted embossing compared to the conventional embossing, and this difference increased with increasing amplitude (Fig. 13a). The edge inaccuracy shows deviations at the edges of the embossing geometries around 15% for the truncated pyramids and around 10% for the spherical cap for all embossed samples. There were no markable differences between the conventional and ultrasonic-assisted embossing results (Fig. 13b).

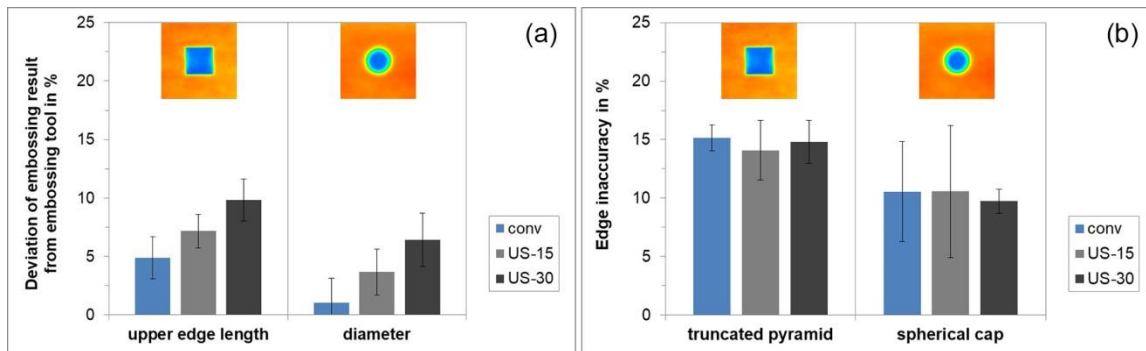


Fig. 13. Deviation of edge length/diameter of exemplary embossed samples referenced to the embossing tool (a) and the edge inaccuracy (b) of truncated pyramids and spherical caps

The differences are caused by tensions within the cardboard sample due to the strong material compression and the different strength properties relating to the grain direction. In the grain direction, the tensile strength properties are higher than cross grain direction, as the fibers have to be stretched or straightened for in-plane deformation to occur. In the cross grain direction, it is mostly the distances between the fibers that changes, which are primarily based on the stretching of weaker fiber bonds. This different forming behavior depends on the grain direction and leads to different types of distortions in the base of the embossing when the load is removed. The comparison of the conventional and ultrasonic-assisted embossing results shows an influence of ultrasound on the curve effect (Fig. 14).

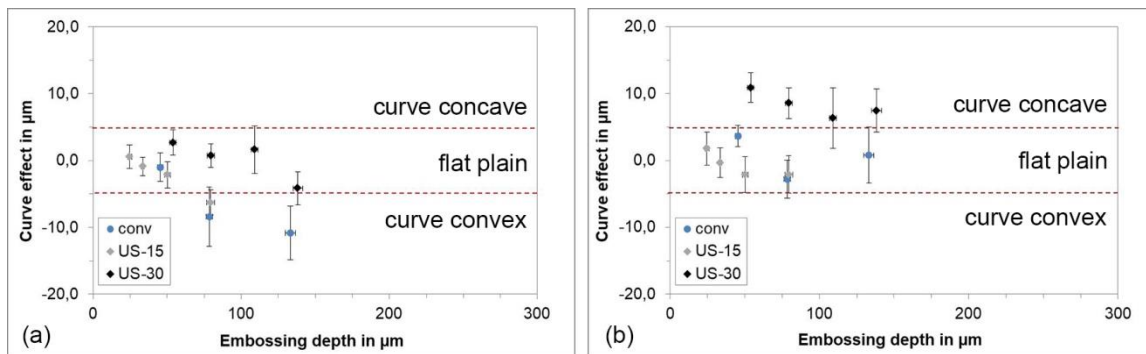


Fig. 14. Curve effect of the embossed samples of truncated pyramids (a) cross and (b) in grain direction

The cross-sectional profiles of the conventional embossed samples cross grain direction mostly showed the base of the embossing had a slight convex curve, with the deepest point occurring towards the center of the embossing. Meanwhile, for the ultrasonic embossing, the values of the curve effect were within the tolerances and therefore were considered to be a flat plain. In grain direction, the base of the conventional and US-15 embossing was flat. However, at the higher amplitude the base had a slight upwards curve, with the highest point towards the center. This curvature was reduced as the embossing depth increased. A direct correlation to the embossing results separated according to the fiber direction could not be proven. The embossing results in grain direction and cross grain direction did not differ significantly (t-test with 5%).

The comparing of cross-section profiles of one embossed sample in grain and cross grain direction visualizes the differences. It provides the height differences between the grain directions and the tensions within the board sample shown in the colored contour plot (Fig. 15). The cross-section profiles intersect in the middle of the embossing and the height differences occur at the edges of the embossing. Due to the symmetrical embossing geometry, the height differences in grain and cross grain direction are limited and not significant.

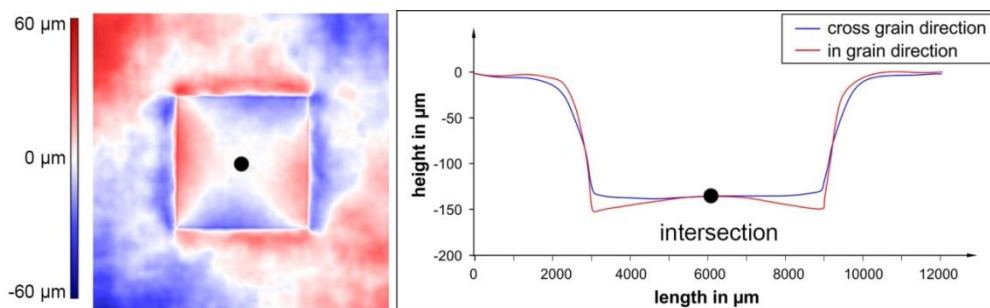


Fig. 15. Differences of forming of an exemplary sample of US-30 cross and in grain direction

Therefore, it can be stated that the differences are caused by tensions within the board sample due to the strong material compression and the different strength properties relating to the grain direction. In the grain direction, the tensile strength properties are higher than cross grain direction, as the fibres have to be stretched or straightened for in-plane deformation to occur. In the cross grain direction, it is mostly the distances between

the fibres that change, and these are primarily based on the stretching of weaker hydrogen bonds. This leads to different types of distortions in the base of the embossing, when load is removed.

When exemplary cross-section profiles of embossed samples with equal embossing depths were compared, there appeared to be no major differences between the conventional and ultrasonic-assisted embossing results (Fig. 16).

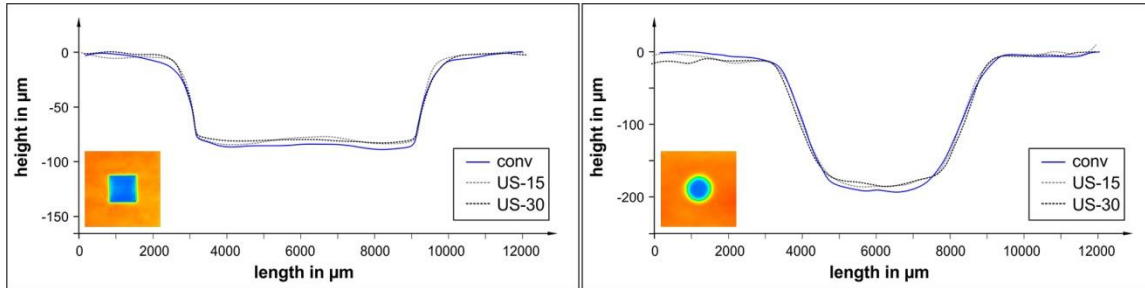


Fig. 16. Cross-sections of exemplary samples embossed with equal embossing heights

However, comparing of cross-section profiles of exemplary samples embossed with equal embossing paths illustrates the impact of ultrasound (Fig. 17). With an equal embossing path, deeper embossing depths are achievable, when the embossing process is assisted by ultrasound.

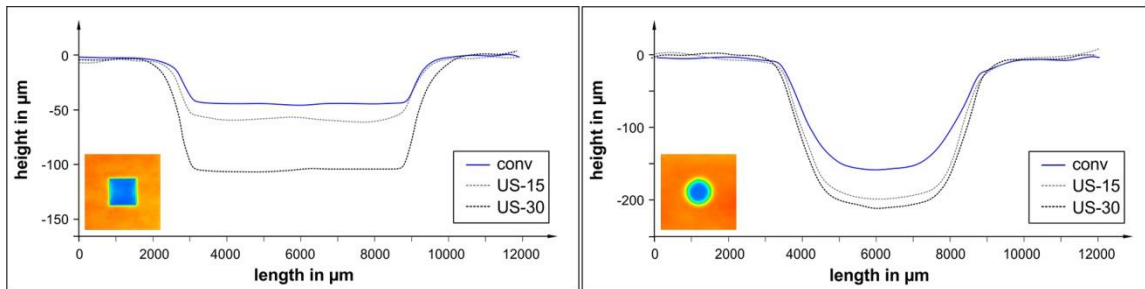


Fig. 17. Cross-sections of exemplary samples embossed with equal embossing paths

In the case of the truncated pyramids, the embossing depth was increased from an average of $45 \mu\text{m} \pm 2 \mu\text{m}$ to an average of $109 \mu\text{m} \pm 2 \mu\text{m}$ for an embossing path of $200 \mu\text{m}$ by the application of ultrasound. For the spherical caps, the embossing depth was increased from an average $133 \mu\text{m} \pm 4 \mu\text{m}$ to $175 \mu\text{m} \pm 12 \mu\text{m}$ for an embossing path of $300 \mu\text{m}$. This was therefore the main benefit of using ultrasound for cardboard embossing.

In summary, the main advantage of ultrasonic-assisted embossing compared to conventional embossing is the reduction of the embossing paths, which requires lower static embossing forces. In addition, higher embossing depths were achieved with comparable embossing paths and the process window can be extended to smaller embossing paths by ultrasonic application. However, the application of ultrasound while embossing leads to higher deviations of the edge length/diameter in comparison to conventional embossing.

CONCLUSIONS

1. The use of ultrasound leads to higher embossing depths for equal embossing paths. Thus, smaller embossing paths are required for comparable embossing depths.
2. Due to the achievable embossing results at lower embossing paths, the application of ultrasound provides an extension of the process window.
3. Due to the dynamic material compression and heating of the material inside, the ultrasound can reduce the re-swelling and increases the efficiency of the forming process.

ACKNOWLEDGMENTS

This work was supported by the German Federation of Industrial Research (AiF/IGF: research project 19717-BR) and the Central Innovation Program (16KN056837) of the Federal Ministry of Economic Affairs and Energy (BMWi). The Keyence 3D-Macroscop was funded by European Regional Development Fund (Europe funds Saxony). The authors acknowledge support by the Open Access Publication Funds of the HTWK Leipzig. The authors are grateful for the support of the University of Applied Sciences Leipzig and the Technical University Dresden.

REFERENCES CITED

- Blechsmidt, J., ed. (2013). *Papierverarbeitungstechnik [Paper Processing Technology]*, München, Hanser Verlag.
- Bos, J. H. and Staberock, M. (2006) *Das Papierbuch: Handbuch der Papierherstellung*, 2nd Ed., Houten, ECA Pulp & Paper.
- DIN EN ISO 534 (2012). "Paper and board – Determination of thickness, density and specific volume," German Institute for Standardization, Berlin, Germany.
- Gmeiner, J. (2001). "Vorrichtung zum Ultraschallverbinden einer mehrlagigen Papierbahn [Device for ultrasonic bonding of a multilayer paper web]," German Patent DE 10252948A1.
- Gmeiner, J., and Schneider, A. (2005). "Vorrichtung zum kontinuierlichen Verbinden und/oder Verfestigen von Materialbahnen mittels Ultraschall [Device for continuous bonding and/or strengthening of material webs by ultrasound]," European Patent EP 1514670A2.
- Grenz, R., and Schramm, S. (2018). "Steuerung der Umformbarkeit faserbasierter Materialien mit hohem Füllstoffgehalt durch den Einsatz festigkeitssteigernder synthetischer Spezialkomponenten [Control of the formability of fibre-based materials with high filler content through the use of strength-enhancing synthetic special components]," (Report No. 09/18). PTS Papiertechnische Stiftung, München, Germany.
- Hauptmann, M. (2010). *Die gezielte Prozessführung und Möglichkeiten zur Prozessüberwachung beim mehrdimensionalen Umformen von Karton durch Ziehen [The Targeted Process Control and Possibilities for Process Monitoring in the Multi-*

- dimensional Forming of Board by Drawing*], Ph.D. Dissertation, Technical University of Dresden, Dresden, Germany.
- Hofmann, A. and Hauptmann, M. (2020). "Ultrasonic induced material compression during the gap-controlled reshaping of dry paper webs by embossing or deep drawing," *BioResources* 15(2), 2326-2338.
- Hünniger, J. (2013). *Untersuchung von Einflussparametern zur qualitätsgerechten Ausformung von neuartigen 3D-Prägestrukturen [Investigation of Influencing Parameters for the High-quality Shaping of Innovative Three-dimensional Embossed Structures]*, Master's Thesis, University of Applied Sciences Leipzig, Germany.
- Jayme, G., and Rosenfeld, K. (1955). "Eigenschaftsänderung von Zellstoff durch Einwirkung von Ultraschall [Change in the properties of cellulose due to the impact of ultrasound]," *Das Papier* 13/14, 296-303.
- Käppeler, U., Huenniger, J., Hofmann, A., Berlich, A. and Engisch L. (2020). "Thermal influence on the mechanical properties of cardboard during an ultrasonic-assisted embossing process," *BioResources* 15(3), 5110-5121.
- Käppeler, U., Huenniger, J., Hofmann, A., Hamblyn, S., Berlich, A., and Engisch L. (2021). "Chemical and morphological changes in fibre structure due to material heating during ultrasonic-assisted embossing of cardboard," *BioResources* 16(1), 5110-5121.
- Laine, J. E., and Goring, D.A.I. (1977). "Influence of ultrasonic irradiation on the properties of cellulosic fibers," *Cellulose Chemical Technology* 11, 561-567.
- Liebau, D., and Heinze, I. (2001). *Industrielle Buchbinderei: Buchfertigung (Serie) [Industrial Bookbinding: Book Production (Series)]*, 3rd Ed., Verlag Beruf + Schule, Itzehoe, Germany.
- Loewe, A., and Hofmann, A. (2017a). "The use and application of ultrasonic vibrations in the 3D deformation of paper and cardboard," *Journal of Materials Processing Technology* 240, 23-32.
- Loewe, A., Hauptmann, M., and Majschak, J.-P. (2017b). "The effect of ultrasonic Oscillation on the quality of 3D shapes during deep-drawing of paperboard," *BioResources* 12(4), 7178-7194.
- Loewe, A., Hauptmann, M., Hofmann, A., and Majschak, J.-P. (2019). "Temperature development of cardboard in contact with high-frequency vibrating metal surfaces," *BioResources* 14(2), 3975-3990.
- Radzanowski, G. (2017). *Untersuchungen zu Strukturveränderungen in Karton im ultraschallunterstützten Prägeprozess [Investigations of structural changes in cardboard in the ultrasonic-assisted embossing process]*, Master's Thesis, University of Applied Sciences Leipzig, Germany.
- Tenzer, H.-J. (1989). *Leitfaden der Papierverarbeitungstechnik [Guide to Paper Processing Technology]*, VEB Fachbuchverlag Leipzig, Germany.
- Turai, L. L. and Teng, C. H. (1979). "Ultrasonic deinking of waste paper – A pilot plant study," *Tappi Journal* 62, 45-47.
- Wallmeier, M. (2018). *Experimental and Simulative Process Analysis of Deep Drawing of Paperboard*, Ph.D. Dissertation, Technical University of Dresden, Germany.
- Wanske, M. (2010). *Hochleistungs-Ultraschallanwendungen in der Papierindustrie – Methoden zur volumenschonenden Glättung von Oberflächen [High power ultrasonic applications in the paper industry - Methods for volume-preserving smoothing of surfaces]*, Ph.D. Dissertation, Technical University Dresden, Germany.

Zahel, M. and Schaffrath, H.-J. (2018). *Steuerung der Schubverformbarkeit und Lagenverschiebbarkeit von Papier und Karton zur Verbesserung der Umformbarkeit [Control of shear deformability and ply shifting of paper and board to improve formability]*, (Report No. 04/2018), PTS Papiertechnische Stiftung, München, Germany.

Article submitted: April 29, 2021; Peer review completed: May 31, 2021; Revised version received and accepted: August 3, 2022; Published: August 22, 2022.

DOI: 10.15376/biores.17.4.5803-5819